Building Research & Information

ISSN: (Print) (Online) Journal homepage: https://www.tandfonline.com/loi/rbri20

Experimental analysis of a prototype for a thermochromic Trombe wall

Arturo Martínez, Carmen Alonso, Fernando Martín-Consuegra, Gloria Pérez, Borja Frutos & Álvaro Gutiérrez

To cite this article: Arturo Martínez, Carmen Alonso, Fernando Martín-Consuegra, Gloria Pérez, Borja Frutos & Álvaro Gutiérrez (2021): Experimental analysis of a prototype for a thermochromic Trombe wall, Building Research & Information, DOI: 10.1080/09613218.2021.1905502

To link to this article: https://doi.org/10.1080/09613218.2021.1905502

Published online: 05 Apr 2021.

BRI BUILDING RESEARCH & INFORMATION
https://doi.org/10.1080/09613218.2021.1905502

Routledge Taylor & Francis Group

Check for updates

Experimental analysis of a prototype for a thermochromic Trombe wall

Arturo Martínez [a], Carmen Alonso [b], Fernando Martín-Consuegra [b], Gloria Pérez [b], Borja Frutos [b] and Álvaro Gutiérrez [c]

[a]Departamento de Construcción y Tecnología Arquitectónicas, Escuela Técnica Superior de Arquitectura de Madrid (Universidad Politécnica de Madrid), Madrid, Spain; [b]Instituto de Ciencias de la Construcción Eduardo Torroja-IETcc (Consejo Superior de Investigaciones Científicas-CSIC), Madrid, Spain; [c]Departamento de Tecnología Fotónica y Bioingeniería, Escuela Técnica Superior de Ingenieros de Telecomunicación (Universidad Politécnica de Madrid), Madrid, Spain

ABSTRACT

Ambitious and innovative refurbishment measures will be required to meet the European Union's goals for limiting building energy consumption. Envelope efficiency can be enhanced, for instance, with new materials and improved passive techniques. Trombe walls (TWs), one such technique, reduce heating demand in winter, although they cause overheating in warm climates. That drawback may be corrected with thermal-optically reversible materials. In this study, a thermochromic mortar was applied to a prototype TW to reduce solar absorption in summer without affecting its wintertime efficacy. Further to field measurements, the maximum surface temperature reached on the wall's thermochromic cladding (TCC) was 32°C in winter and 44.7°C in summer. The indoor cold weather temperature in the module ranged from 7.9°C to 16.5°C for a mean of 11°C, compared to 25.1°C to 32.2°C with a mean of 28.9°C in warm weather. Ventilating the air gap at 60–200 ach prevented the cladding from fading to nearly colourless in winter. In light of the improved thermal transfer performance delivered, the TTW proposed can profitably be used for energy refurbishment in existing buildings.

ARTICLE HISTORY
Received 14 July 2020
Accepted 15 March 2021

KEYWORDS
Thermochromic Trombe wall; energy refurbishment; solar control technology; chromogenic mortar

Introduction

In its response to the energy crisis, the European Union (EU) has put forward a battery of measures to reduce energy consumption in buildings, which it has identified as one of the continent's most energy-intensive areas. Environmental control accounts for 50% of the energy consumed in Europe, 80% of which to heat and cool buildings (Recomendación de la Comision de 7.6.2019 relativa a la modernización de edificios, 2019). In pursuit of cleaner and more efficient energy use, the EU encourages the installation of passive systems to lower building energy demand while ensuring user comfort levels (Directiva (UE), 2018/844, 2018).

In passive environmental control systems solar radiation stores and transfers heat energy as needed. Trombe walls (TWs), presently the most widespread and thoroughly studied of such systems (Bellos et al., 2016), conventionally consist (in the Northern Hemisphere) in a thermally massive southward-facing wall with openings at the top and bottom for convection. Glass siding at a certain distance from the wall creates a tight air space or pocket. As the wall accumulates solar radiation, it transfers heat to the pocket by convection. The heated air then flows indoors across the upper opening while the cold indoor air flows outward into the pocket at the bottom. The wall's dark outside finish increases solar absorptance for more effective capture of solar energy (Bevilacqua et al., 2019). In blank walls with no insulation, the heat accumulates and is transferred inward by conduction and radiation.

Most of the studies conducted on TWs to date have focused on improving energy accumulation and heating performance with the use of materials such as water with greater thermal mass (Liu et al., 2013; Nayak, 1987) or phase-change potential (Zalewski et al., 2012). Although initially designed for continental climates with low cooling demand, given their efficient contribution to indoor heating in cold weather, low cost and convenient geometry, TWs have gradually come into more widespread use (Bevilacqua et al., 2019). In warmer climates such as prevailing in Mediterranean countries, however, TWs may cause overheating even outside the summer season.

A number of authors have sought solutions to that problem based on the use of shutters or blinds or different types of ventilation. Depending on the type of glazing, Stazi reduced cooling demand by 42% to 48% with roller shades (Stazi et al., 2012). In 2019, Bevalacqua

CONTACT Arturo Martínez arturo.martinez.garcia@alumnos.upm.es

lowered cooling demand by 36.1% with different ventilation strategies and vertical shades (Bevilacqua et al., 2019). Bajc covered the outer side of a TW with photovoltaic slats that generated heat energy while also establishing an indoor summertime temperature of 29.8°C (Bajc et al., 2015). Dabaieh and Elbably, in turn, reduced heat gains in a TW by 70% by placing a sunshade with a reflecting surface over the glazing (Dabaieh & Elbably, 2015). Stazi contended that TWs should not be used in Mediterranean climates without solar protection (Stazi et al., 2012), although such protection raises the costs and complexity of refurbishment (Pittaluga, 2013). Drawing from 'living lab' findings, Dabaieh concluded that occupants must be willing and able to manually control solar protection, including opening and closing curtains and shades (Dabaieh & Elbably, 2015). And Beck pointed out that roller shades may malfunction (Beck et al., 1993).

Innovative components for solar control have been developed thanks to technological research. When duly activated, so-called dynamic or adaptable materials can reversibly change their thermal-optical properties. Chromogenic (electrochromic, gasochromic, photochromic and thermochromic) glass is the most widespread of those materials (Baetens et al., 2010). In 2015, Reynisson found that a room with an electrochromic window activated in summer saved 10% to 30% more energy than one with adjustable shades and 50% to 75% more than an unprotected opening (Reynisson & Guðmundsson, 2015). One of the strategies suggested by Camacho-Montano to reduce solar gains and hence overheating in school buildings consists in fitting them with electrochromic glass (Camacho-Montano et al., 2020). Thermo-optically variable materials are not limited to glazed elements, however.

High reflectance 'cold' paint may also lower cooling loads in summer. Some of the samples studied by (Zinzi, 2016) raised near infrared (NIR) reflectance by 475% relative to the initial value. Simulation studies have shown that under certain circumstances cold paint can lower a building's cooling demand by around 19%. The final energy balance is negative or scantly significant in such cases, however, due to the adverse effect on heating, for as reflectance remains the same in the cold season, cold cladding or surfacing reflects the solar radiation required when temperatures drop. In a recent study, Fabiani observed dynamic cladding to perform better than cold surfacing (Fabiani et al., 2020). The author's simulation showed that in a well-insulated building, both thermochromic and cold paint could lower envelope surface temperature by up to 10 K more in warm weather than conventional dark paint. In the cold season, however, whereas absorptance rose in the chromogenic surfacing to equal that of conventional dark paint, cold paint maintained its albedo. The resulting surface temperature was 4 K lower than in the other two types of coating.

Very few authors have explored chromogenic materials in conjunction with Trombe walls. In 1993, Beck analysed water-based thermochromic polyether and ethylene oxide group gels placed between two panes of glass along with a gelling agent to lower solar radiation in solar-based systems such as TWs (Beck et al., 1993). In 2013, Pittaluga simulated the use of electrochromic glass to lower summertime solar radiation on a TW. The findings showed the electrochromic TW saved 17.6% more energy than a standard wall and 29.5% more than a conventional TW (Pittaluga, 2013). Other studies have explored non-glazed chromogenic materials for use in TWs. In 2014, the Eduardo Torroja Institute for Construction Science (IETcc) initiated research on a thermochromic mortar that changes its optical properties at a certain surface temperature to control solar absorption (Perez et al., 2018). More specifically, when exposed to low temperatures the mortar adopts a dark tone associated with low reflectance (high absorption), but when temperatures hit a certain target, raising reflectance, it turns colourless. In 2018, those studies were refocused to explore the use of the chromogenic mortar as cladding on a thermally massive TW in a region characterized by warm summers (Perez et al., 2019). Given its chemical composition, the resulting thermochromic Trombe wall (TTW) can modify its absorptance and reflectance to control the solar radiation received and improve thermal performance. When developing the respective thermochromic cladding (TCC) Garhasbi's recommendations were followed to block the wavelengths that prompt photo-deterioration (Garshasbi & Santamouris, 2019). A simulation run to find the activation temperature showed that the material clarified or faded at an activation temperature of 30°C to 31°C, i.e. the target temperature at which wintertime absorption (attendant upon what is hereafter referred to as 'coloured' conditions) and summertime reflection (hereafter 'colourless') were balanced (Martín-Consuegra et al., 2019).

This study, conducted in Madrid, Spain, was designed to determine whether the thermal behaviour of conventional TWs in regions with warm summers can be improved with thermochromic mortar cladding, i.e. materials that fade to nearly colourless when heated. The thermochromic Trombe wall (TTW) prototype used in this experiment was also analysed to determine the effect of radiation and outdoor temperature on its performance. A third factor studied was related to the rise in solar radiation (anticipated for the reasons discussed in the Introduction) to the activation temperature even in the wintertime. To address that issue, the system was fitted with controlled ventilation for testing in the absence of the colour loss that would adversely affect TTW heating efficiency.

TTW prototype

The TTW prototype described below was built at the Technical University of Madrid's Montegancedo campus in a test cell under monitored weather conditions (Martín-Consuegra et al., 2019). This article analyses the experimental data found for the prototype, characterizes its thermal behaviour and determines its adaptability to existing buildings.

The prototype wall analysed had a $2.16 \times 2.16\ m^2$ façade made (from the outer-most to inner-most layer) of the following elements: a (4 mm + 4 mm) laminated, yellow-tainted glazed window framed in painted white wood; a 200 mm air space; thermochromic (TCC) mortar cladding consisting in $300 \times 300\ mm^2$, 1 cm thick panels laid on a 20 mm layer of sand-cement; a 115 mm perforated brick wall; a 50 mm non-ventilated pocket; and a 40 mm hollow brick partition wall (Martín-Consuegra et al., 2019) (Figure 1). The glazing was tainted yellow to minimise wavelength transfer between the ultraviolet range up to 433 nm and protect the TCC from solar radiation-induced deterioration (Perez et al., 2019).

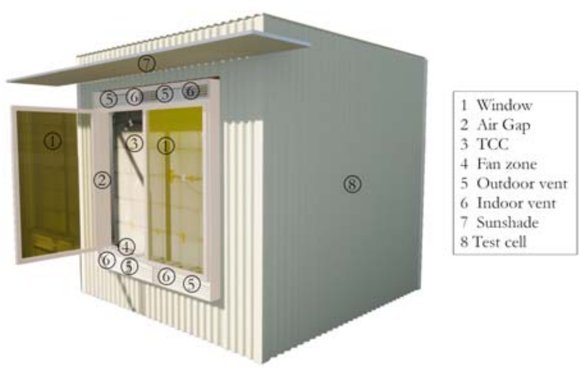

Figure 1. TTW prototype components.

The window joinery and composite wall bore openings for the air to circulate as programmed in winter and summer (Figure 2), fitted with $150 \times 450\ mm^2$ mechanized grated vents that opened or closed depending on the season. Two of the four vents connecting the air space to the outdoor air were located at the bottom of the window and the other two at the top. Openings with similar dimensions and positions but penetrating across the entire composite wall, connected the space to the indoor environment.

According to Gavira, TTWs should not face south, for as the solar radiation deriving from that orientation heats the TCC to above the activation temperature, the rays needed for heating are reflected off the wall (Gavira et al., 2018). To compensate for that drawback without foregoing the solar potential of a southern orientation, in this experiment seven fans were installed in the air space to reduce the TCC surface temperature. The first fan was triggered when the thermocouples on the TCC surface detected a temperature of 25°C. Two more fans were tripped at 26°C, two at 27°C and the last two at 28°C. A 700 mm wide sunshade was

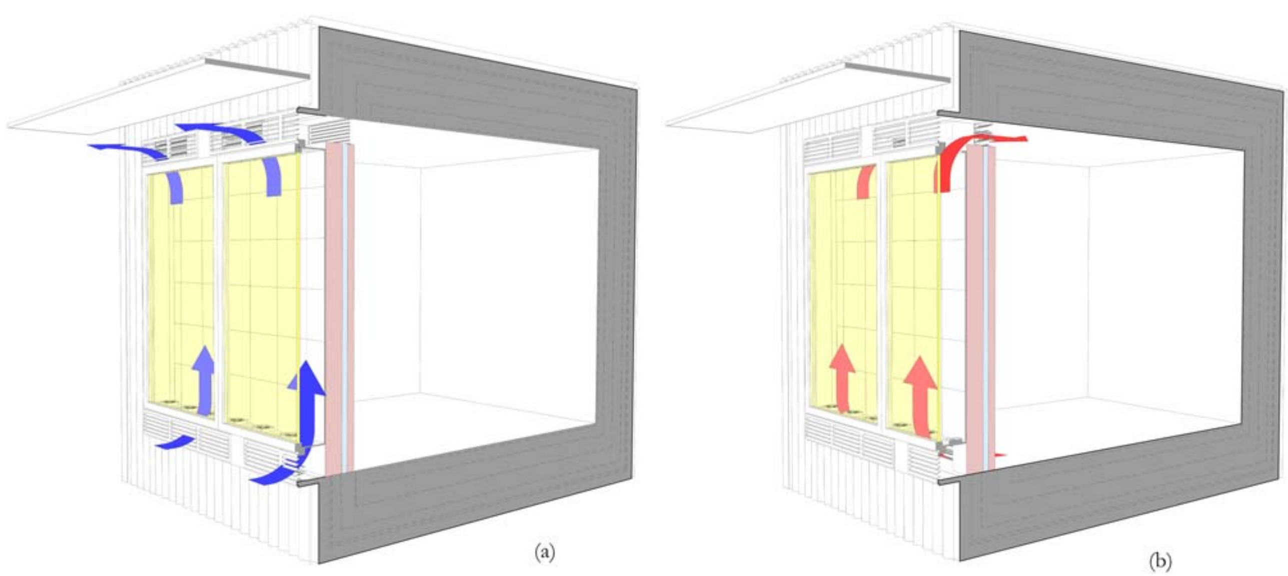

Figure 2. Vent positions: (a) summer; (b) winter.

positioned width-wise across the entire façade at 40 cm above the window to block direct solar radiation in the summer but allow for full solar capture during the winter solstice.

Methodology

In the experiments conducted to determine the effects of (temperature-induced) changes in TCC absorptance and reflectance on the TW, indoor temperatures were taken by a sensor inside the module or cell and surface temperatures by thermocouples installed on the air pocket side of the cladding. A pair of anemometers measured air velocity between the glass and the masonry wall. All data were recorded at 10 min intervals. Improvements in the indoor conditions were assessed in terms of pre-defined winter and summer time comfort ranges.

TCC: optical properties

Thermochromic pigments, normally micro-encapsulated powders or slurries, reversibly change colour when exposed to heat. They are used in a variety of materials for applications ranging from brand protection to building cladding, as proposed in this study. Colour change is typically set to an activation temperatures of 15°C, 31°C or 47°C. The thermochromic cladding (TCC) analysed is a cement-based cladding bearing organic microencapsulated pigments that reversibly change its optical properties at an activation temperature of 31°C. Pérez (Perez et al., 2018), studying this material at above (40°C) and below (20°C) the activation temperature, found its reflectance in the 350 to 800 nm range to be higher when colourless than when coloured and similar in the rest of the spectrum. The optical properties of the thermochromic mortar panels specifically prepared for this study were determined after securing the cladding to the TTW. Measurements were made on the coloured panels on 18 December 2018, one day prior to the early winter week whose results are analysed and recorded as the condition prevailing in that week (19–25 December 2018), as well as in the absence of sunlight in the late winter week (08–14 March 2019). TCC reflectance in the colourless panels, measured in warm weather, was found to remain essentially constant throughout the summer (Figure 3). The five absorptance/reflectance readings taken under these three conditions, one on each of the four corners and one in the centre of the thermally massive wall, were recorded in the 300 to 1750 nm range with a Stellarnet handheld fibre optic spectrometer fitted with an Ocean Optics 50 mm integrating sphere. Visible and solar reflectance and absorptance were determined as recommended in Spanish and European standard UNE-EN 410. Although the measuring range specified in that standard extends to 2500 nm, 95% of the total solar energy falling on the Earth's surface lies in the 350–1700 nm range, and 96.6% in the range applied here. The absorptance and reflectance measurements for the TCC used in this study are listed in Table 1.

TTW monitoring

TTW performance was monitored in real time with sensor nodes that recorded the data needed to analyse system performance in the conditions prevailing in summer and winter: TCC surface temperature; air temperature inside the module; air flow velocity; outdoor air temperature, relative humidity, air velocity

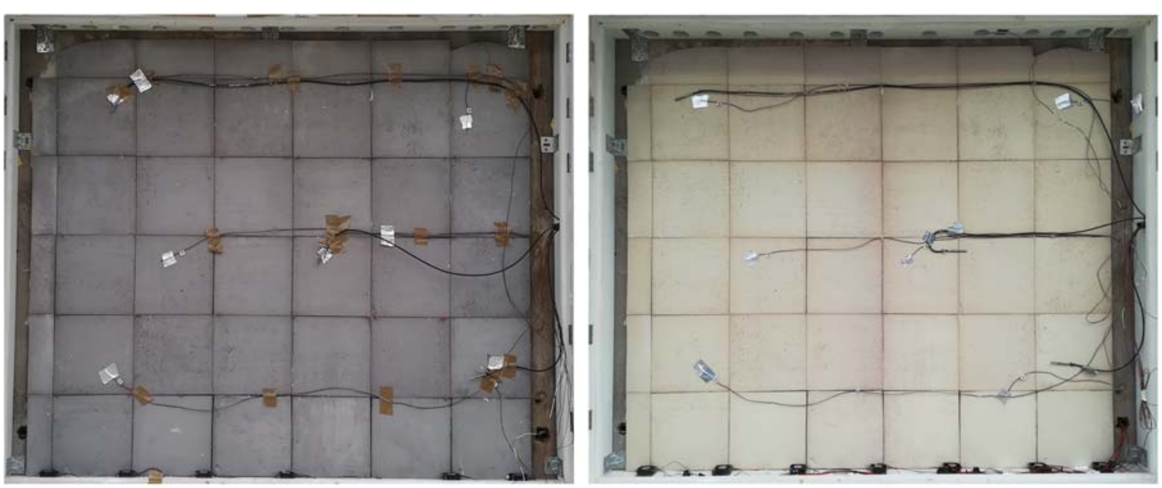

(a) (b)

Figure 3. TCC colour tones (a) dark; (b) light.

Table 1. TCC absorptance and reflectance measurements.

	Colourless		Coloured	
	Solar	Visible	Solar	Visible
Absorptance	0.36	0.47	0.43	0.58
Reflectance	0.64	0.53	0.57	0.42

and direction; horizontally incident solar radiation; and atmospheric pressure. The energy consumed by the environmental control facility was likewise measured and recorded. In addition, the TTW was fitted with seven 12 V fans featuring a nominal airflow of 26.63CFM each that were switched on automatically and by stages to keep the TCC from overheating when the pre-defined target temperatures were reached.

The nodes gathered indoor and outdoor wall surface temperature and the air temperature inside the TTW (Figure 4), both to a precision of 0.1°C, from 24 type T thermocouples, the fan-induced air flows in the pocket from three air velocity transducers and the meteorological conditions from a meteo station sited in a nearby test module. This article reports only on the seven thermocouples located on the outer side of the thermochromic mortar panels (T13 to T19) and two of the air velocity transducers (A2 and A3) positioned on the same surface. In this real-time data acquisition system designed to an ad hoc embedded arrangement consisting in RS-485 serial bus-interconnected nodes, each node collected information from all the sensors to which it was connected at 10 ms intervals. The mean calculated for the last 100 measurements was stored second-by-second and subsequently relayed to the main controller further to a Modbus RTU RS-485 protocol.

The Linux operating system-run main controller, a microcontroller with a UPS circuit connected to the nodes by an electronic carrier, acquired all the data in the nodes at 10 min intervals and stored them on a built-in SD card along with the acquisition date and time. All that information was then immediately forwarded to the monitoring server, where it was synchronized and where the electrical were converted to physical units and periodic scripts were run to process and upload the data to the monitoring database. The OS likewise gathered and averaged the surface temperatures (ΔT) recorded by thermocouples T12 to T19, switching the fans on to control the temperature on the TCC surface in keeping with the criteria set out in Table 2.

The monitoring server synchronised all the data, converting electrical to physical units and running periodic scripts to process and upload the data to the monitoring database. The data used in the analysis described in section 5 were collected from 12 December 2018–30 September 2019, although monitoring is ongoing at this writing.

The data recorded included surface temperature on the TCC, air temperature inside the module, energy consumption by the environmental control facility and air flow velocity. Outdoor air temperature, relative humidity, air velocity and direction, solar radiation in the horizontal plane and atmospheric pressure were also recorded at a meteo station sited in a nearby test module.

Thermal comfort range calculations were performed with IWEC meteorological data drawn from station No. 082210 using the *Climate consultant software*. The coefficients adopted were: met activity, 1.1; clothing, 1.0Clo in winter and 0.5Clo in summer, predicted percentage dissatisfied (PPD), 10%. Optimal wintertime comfort temperature was defined as 22.1°C, within a range of 20.3°C to 24.3°C. The difference in the clothing coefficient between winter and summer, accommodated

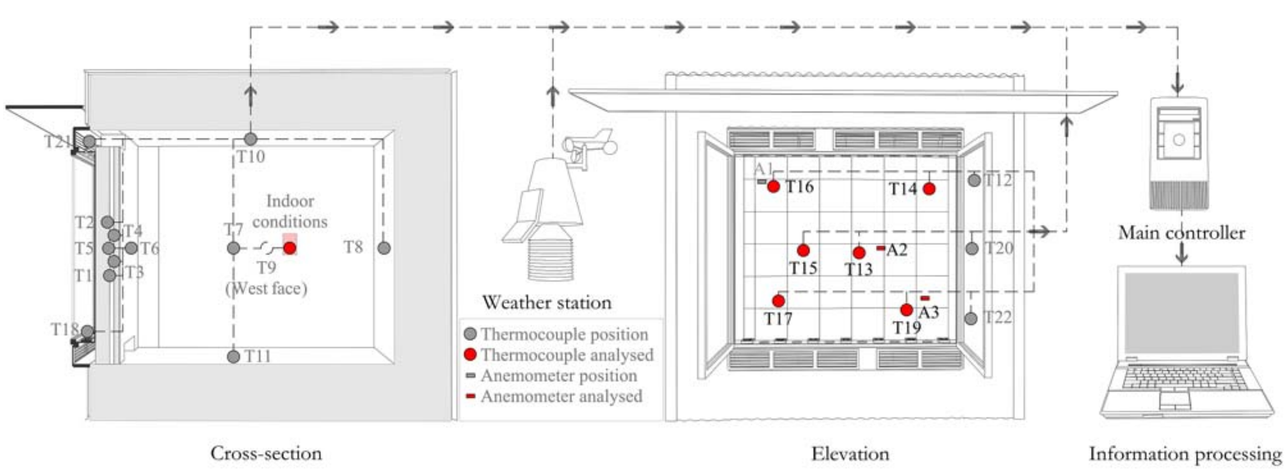

Figure 4. Positions of surface thermocouples (T) and anemometers (A).

Table 2. Criteria for switch the fans on.

If $\Delta T > 28°C$	Then	switch on 7 fans
If $28°C > \Delta T > 27°C$	Then	switch on 5 fans
If $27°C > \Delta T > 26°C$	Then	switch on 3 fans
If $26°C > \Delta T > 25°C$	Then	switch on 1 fan
If $\Delta T < 25°C$	Then	switch on 0 fans

by the model, translated into an optimal summertime range of 23.8°C to 26.7°C.

The hours of thermal discomfort (DH) were computed as the sum of the hours indoor cell temperatures lay outside the comfort range, referred to here as overheating when they exceeded 26.7°C and supercooling when they dropped below 20.3°C. The parameter discomfort degree-hours, found as the sum of the degrees of temperature over or under the limits defined, was used to determine the comfort afforded by the TTW relative to outdoor conditions. The efficacy of the chromogenic mortar compared to conventional cladding was found by simulation based on DDH.

Periods analysed

The analysis described in section 5 was based on information collected from 12 December 2018–30 September 2019, although monitoring is ongoing at this writing. Three weeks representative of the passive and active conditions during the 9 month data collection period were selected to analyse the TTW prototype in warm and cold weather (Table 3). The criteria for defining representativeness were the presence of conditions in keeping with the season and TCC optical stability (Table 4). The winter period was chosen on the grounds of irradiation and temperature variability to assess the effect of those parameters, including high values to test whether ventilation prevented thermochromic material fading. A week when high irradiation and temperature values were recorded was chosen to represent the summer season to determine the least favourable indoor conditions. The conditions prevailing in the 3 weeks are described below.

Table 3. TTW and experimental cell settings.

Week	Period	Vent setting	Environmental control
1	19–25 December	Winter	No
2	8–14 March	Winter	Heating
3	8–14 July	Summer	No

Table 4. Outdoor weather conditions during the weeks chosen for analysis.

Week	Mean outdoor temp (°C)	Max outdoor temp (°C)	Min outdoor temp (°C)	Mean wind velocity (Kmh)	Max irradiance (W/m^2)
1	7.0	17.5	1.5	1.6	535.0
2	11.9	24.5	−0.2	2.8	823.2
3	27.0	38.6	14.6	3.8	847.2

- Week 1, 19–25 December, the heating season. The vents were positioned in the 'winter' setting (outer closed and inner open). No additional heating was provided to analyse the behaviour of the system, deemed for these intents and purposes to be a conventional TW to which the TCC was attached.
- Week 2, 8–14 March, end of the heating season during which the system was set for 'winter'. Heating was activated in this period when the indoor temperature dipped below 21°C to quantify active heating energy consumption with the TTW in place.
- Week 3, 8–14 July, the cooling season. The vents were set for 'summer' (outer open, inner closed); no environmental control system was activated. The purpose was to analyse the TW as a ventilated façade in which system thermal gain would be lowered by the reflection of the sun's rays off the TCC surface and the air space ventilation strategy.

Results and discussion

This section discusses and analyses the TTW monitoring data, including TCC surface temperature, air velocity inside the air space and indoor compared to outdoor temperatures in the 3 weeks studied. The heating energy consumed in week 2 is also discussed.

Passive setup in the heating season: week 1

This sub-section discusses the week 1 findings by the three parameters studied: surface temperature, air velocity and indoor temperature.

Surface temperature

In addition to the TTW surface temperatures during the week, Figure 5 plots indoor and outdoor temperature, the temperature in six thermocouples (T13 to T17 and T19) and radiation, graphically depicting the close correlation among them. The activation temperature and the target temperatures at which one, three, five or seven fans were triggered are also shown. The highest outdoor temperature was 17.7°C and the lowest 1.5°C. Peak solar radiation was recorded on the last three days. The thermocouples on the TCC and the sensor inside the module recorded the temperatures graphed in Figure 5. Both were most stable on the third and

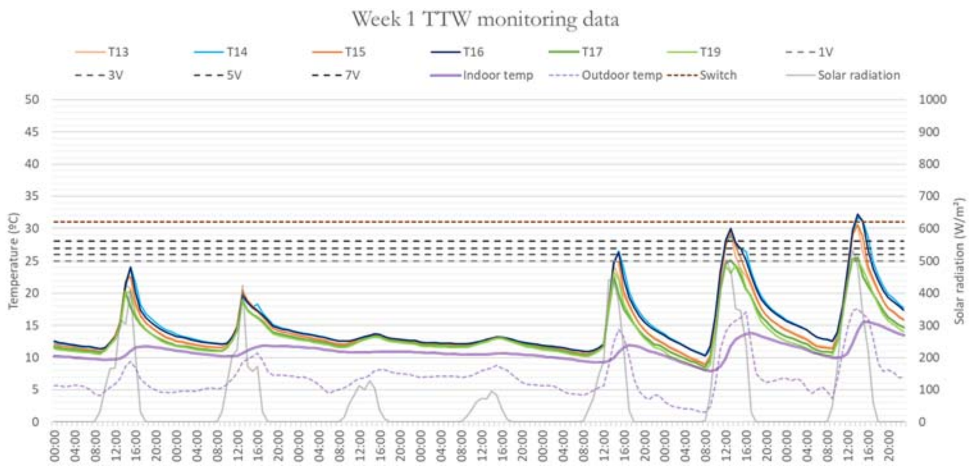

Figure 5. Week 1 TTW monitoring data.

fourth days, when solar radiation was weakest. In contrast, peak radiation, 535 W/m^2, was recorded on 25 December at 13:00, followed 1 h later by the highest surface temperature readings, recorded in upper wall thermocouples T14 (31.7°C) and T16 (32.2°C). Two hours later (16:00) the indoor temperature peaked at 15.6°C, the week's highest value, although the outdoor temperature was even higher, at 16.1°C. Including that hour, in the period from 14:00–21:00 the indoor temperature ranged from 14.1°C to 15.6°C even though the outdoor temperature dropped from 17.6°C to 7.7°C. In other words, the wall's thermal inertia prevented the steep decline in the outdoor temperature from affecting the indoor environment.

The mean temperature recorded by the thermocouples was 14.4°C. Although radiation declined abruptly every day of the week at 16:00, the decrease in wall surface temperature was delayed by the TTW's capacity to accumulate heat. Vertical stratification was observed in the wall. Upper thermocouples T14 and T16 recorded the highest temperatures during the week, with means of 15.2°C and 15.1°C, respectively, whereas the two lowest means and the week's lowest temperatures were recorded at the base of the wall. The mean at T17 was 13.6°C and the low 8.5°C, whereas the mean at T19 was 13.4°C and the low 8.0°C. These findings indicate that at greater height, greater thermal gain. Consequently, the air in the room flowing into the air space through the lower openings was heated as it rose, inducing a rise in upper wall temperature. That behaviour has been proven graphically in earlier studies (Hernández-López et al., 2016).

The thermocouple temperatures were clearly below the Tc in the first 6 days of the period and exceeded the target at T16 by 1°C at 14:00 on the last day. TTW behaviour could therefore be likened to that of a coloured wall with a uniform, constant optical response characterized by the respective reflectance curve. More specifically, visible absorptance was 0.58 and the solar value 0.43.

Air velocity in the air pocket

Air velocity in the air pocket was naturally affected by fan operation. Programmed to come on when the mean temperature in the thermocouples exceeded 25°C, these elements were activated during only 3 h in the first week. Five operated on day 6 and seven on day 7 (see in Figure 5 the position of the peaks on the thermocouple temperature plots relative to the 5-fan and 7-fan trigger temperatures). In the rest of the week, the fans remained off. Anemometer A2 recorded a mean velocity of 0.07 m/s, peaking at 0.14 m/s, and anemometer A3 a mean of 0.04 m/s and a maximum of 0.20 m/s. Both peaks were reached on the last 3 days of the week and observed to concur with the highest solar radiation values: 441.5, 505.17 and 517.0 W/m^2 (Figure 6). When radiation was lowest, on days 3 and 4, velocity was stable. The inference here is that air velocity and solar radiation tended to follow a similar pattern.

That notwithstanding, in the first 5 days, A3 recorded scant or no air velocity, which only rose with the peaks in radiation, whereas A2 recorded greater air velocity and turbulence, even during periods with no solar radiation. In the absence of forced ventilation in the air space, the difference between the two anemometer readings may be attributed to their position on the TCC surface (Figure 7). A2 was located on the vertical axis of one of the lower openings in the thermally massive wall at a greater height than A3. The air from the module flowed through that opening and then upward. Moreover, TCC-induced convection heating in the rising air raised velocity even further. In contrast, A3 was positioned

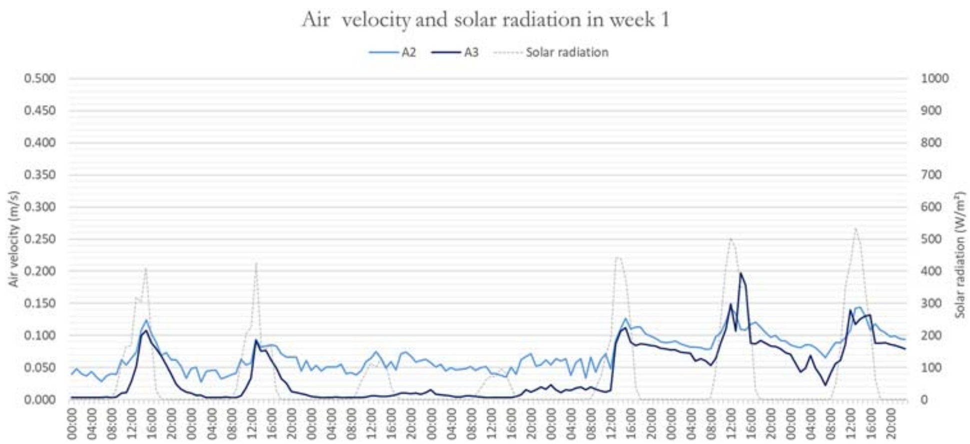

Figure 6. Air velocity and solar radiation in week.

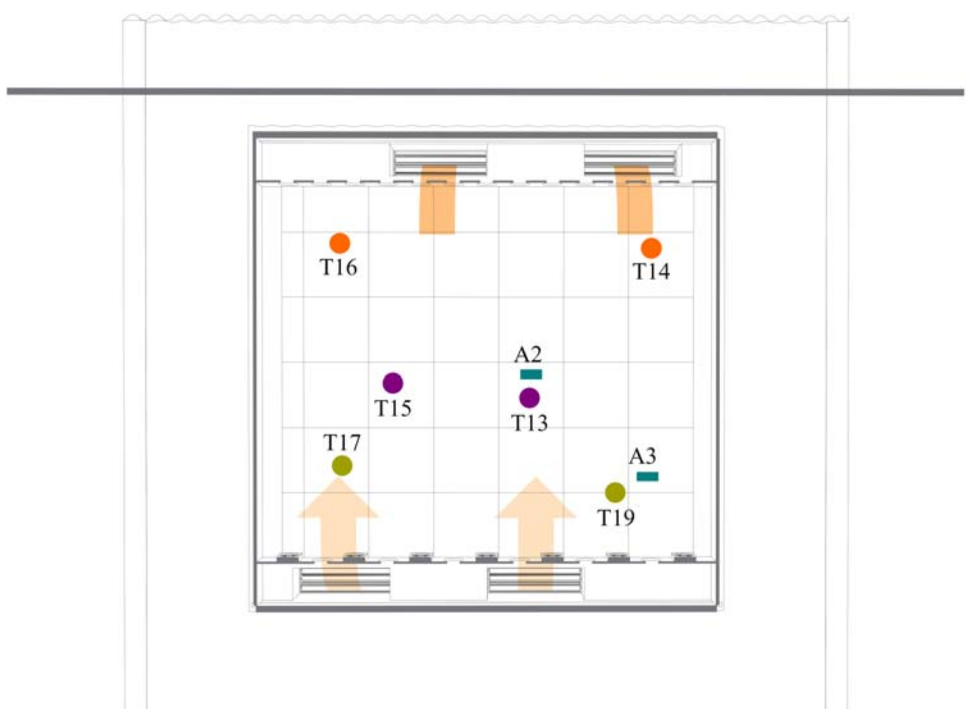

Figure 7. Vent positions in the massive wall.

lower and on the right corner of the wall, outside the pathway of the air flowing through the lower openings.

Indoor vs outdoor temperatures

The mean TCC surface temperature shown on the graphs in Figure 5 was calculated as the mean of the surface thermocouple readings. Solar radiation and outdoor temperature were deemed the prevalent weather conditions. The indoor temperature in week 1 ranged from 7.9°C to 15.6°C, for a mean of 11°C. The lowest values were recorded on day 6, when the TTW kept the indoor temperature at 8.1°C, compared to an outdoor value of 1.5°C. The indoor environment was 4°C warmer on average than the outdoor air. On days 3 and 4, with little sun, the outdoor temperature fluctuated from 4.5°C to 8.8°C, whilst inside the module the temperature declined by only 1.5°C in that period, from 11.7°C to 10.3°C. Day 7 was the warmest, at 17.7°C, and also exhibited the highest solar radiation (535 kWh). As a result, the highest TCC surface and indoor temperatures were also recorded on that day. The outdoor temperature began to decline 2 h after peaking, by 4°C in just one hour, and continued downward to 6.9°C at the end of the day. In the same period the indoor temperature in the module held at approximately 15°C for 5 consecutive hours, declining to

14°C for around 3 h and to 13.5°C at the end of the day (Figure 8).

TTW thermal capture, accumulation and transfer mitigated the extreme outdoor conditions. Even on sunless days, the records showed scant heat loss. Although the winter temperatures were below comfort levels, the stability of the curve in Figure 8 shows that using a TTW with an active heating system would be energetically beneficial. Although indoor comfort as defined by the aforementioned ranges was not attained inside the cell at any time during this first week, an analysis of the temperatures recorded hourly shows that the TTW reduced DDH by 15%. One of the limitations to this experiment, however, was that the cell was not inhabited and consequently not subject to other thermal loads that would have induced variations in the indoor temperatures.

Active heating season, week 2

In week 2, from 8 to 14 March, the electrical heaters were connected and set to come on at a target temperature of 21°C. As ventilation to prevent colour fading in the thermochromic mortar was designed for passive conditions (no environmental control), it was unsuitable in an active heating setup. Consequently, the efficacy of the ventilation system proposed to avoid colour loss of the TCC was not analysed in week 2.

Surface temperature

As Figure 10 shows, in week 2 TTW surface temperature also moved in step with the other parameters graphed. The mean outdoor temperature in week 2 was 11.9°C. All days were sunny, with much higher solar radiation than in week 1 and a maximum daily mean of 784.74 W/m^2. The mean temperature recorded in the surface thermocouples was 23.2°C. The highest means were found in T13 (25.5°C) and T17 (24.5°C), with T13 peaking at 45.9°C. The lowest means were recorded by T15 (located on the same area of the wall as T13), at 22.2°C, and T19 (same area as T17), at 24.5°C. During the week the eaves protected the TCC from solar radiation at certain times and in certain areas (Figure 9), which would explain the difference in the values recorded by the uppermost thermocouples, T14 and T16. On day 7 the outdoor temperature declined to −0.2°C, directly impacting TCC surface temperature. In T19 it dropped to 9.9°C (Figure 10).

Beginning on day 2, thermocouples T13 with 45.9°C and T17 with 39.4°C exceeded the mortar Tc for nearly 8 h. Upper thermocouples T14 and T16 exceeded the Tc only on days 3 and 4 and for no more than 2 h, at values of under 32°C. T15 exceeded Tc on days 2–5 with a peak temperature of 33.4°C, whereas T19 recorded > Tc temperatures on days 3–5 for 2 h to 4 h, with a peak of 32.7°C. Those data denoted substantial differences in duration and temperatures recorded by mid-height

Figure 9. Shade from the eaves on TTW, 8 March 2019 at 14:00.

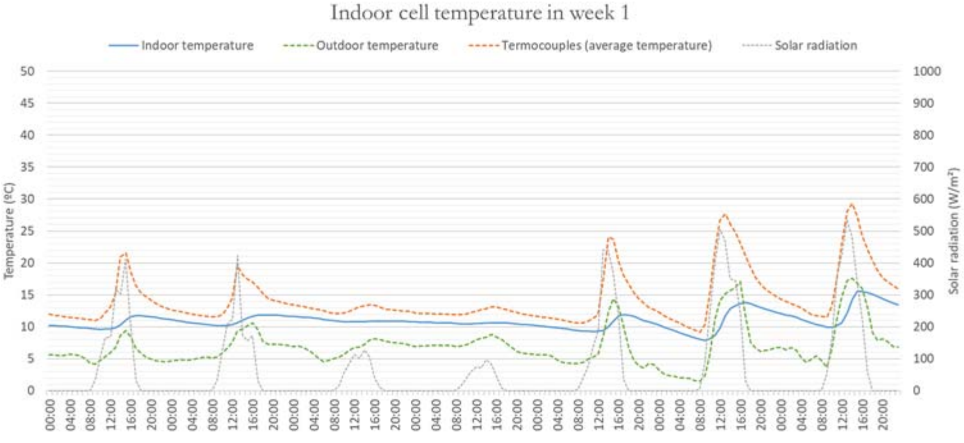

Figure 8. Indoor cell temperature in week 1.

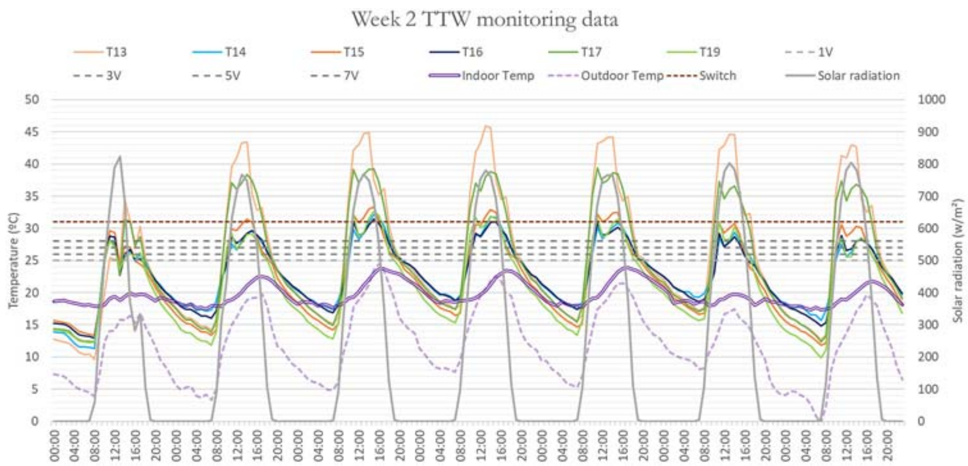

Figure 10. Week 2 TTW monitoring data.

thermocouple T13 and lower wall T17. During the day the shade afforded by the eaves had a greater effect on the upper part of the thermally massive wall, inducing lower readings in thermocouples T14 and T16. The considerably higher surface temperature in thermocouples T13 and T17 might be attributable to their position on the same vertical axis as the lower air space openings (Figure 7). In contrast to week 1, in week 2 when the indoor module temperature was under 21°C the heating switched on and the air was heated before flowing into the air space. When flowing upward in the space from the lower openings its temperature rose even more due to TCC-induced convection heat, prompting the thermocouples along the vertical pathway to record much higher temperatures. That would explain why the T19 and T15 readings were not as high, despite receiving the same amount of radiation. That reasoning is further supported by the fact that the surface temperature peaked in T13 and T17 when the heating had been on for 6–15 h.

Air velocity in the air gap

Anemometer A2 recorded a mean velocity of 0.08 m/s, peaking at 0.24 m/s, and anemometer A3 a mean of 0.12 m/s and a maximum of 0.32 m/s. The greater air velocity relative to week 1 was due to fan operation. The fans switched on every day at 10:00 and remained on for 7–10 h (Figure 10). Whereas A3 recorded increased air velocity, A2 velocity and turbulence readings were lower and unrelated to fan operation (compare Figures 10 and 11). As lower wall A3 was positioned near the fans it was more susceptible to the air flows generated, which declined in speed or even dissipated altogether before reaching A2. That would explain the difference in behaviour between the two sensors.

Indoor vs outdoor temperatures

The mean indoor temperature in week 2 was 19.6°C, compared to the outdoor mean of 11.9°C. As the heating was triggered at temperatures of under 21°C, the indoor

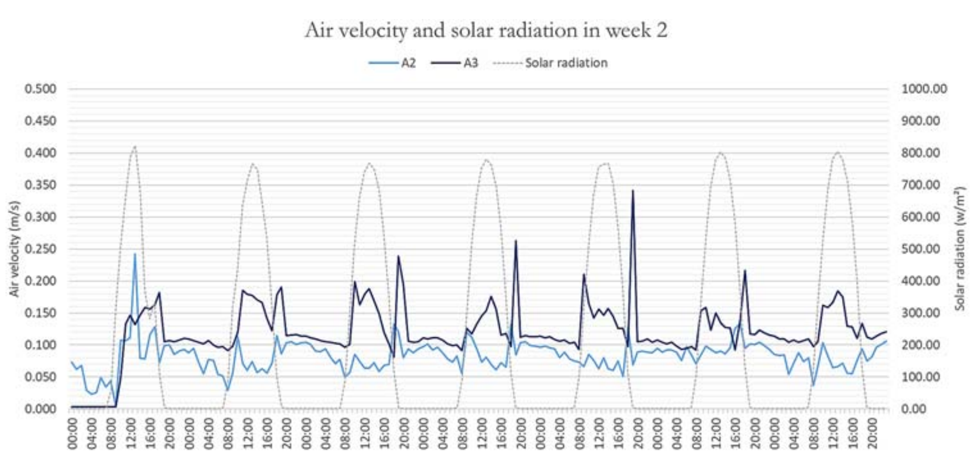

Figure 11. Air velocity and solar radiation in week 2.

temperature ranged from 17.4°C upward. The heating came on from 11:00–13:00. When the target temperature was exceeded, it switched off and mortar thermal behaviour was determined by radiation and the outdoor temperature (Figure 12). Even though the TCC surface temperatures exceeded the activation temperature for several hours on the last 6 days of the week, inducing colour loss in the cladding, the indoor temperature remained at 18.9°C to 23.7°C for 2–4 h after the heating switched off. Indoor temperatures were impacted by heating system operation, however, and should be analysed against the backdrop of electric power consumption.

Power consumption

A mean 62.44 Wh was consumed in week 2. Substantially more power was consumed on day 7, with a mean of 87 Wh, followed by day 2 with 75 Wh. Consumption peaked at 223.3 Wh on day 7 at 07:00, when the week's lowest temperature (−0.2°C) was recorded. Outdoor temperatures did not rise as far on day 6 as on the preceding 4 days. As a result, the heating remained on for 27 consecutive hours in that period, inducing the aforementioned peak consumption. The power peak recorded on day 2 was somewhat lower, induced by outdoor temperatures of 3°C to 5°C. Lowest consumption, at 35 Wh, was observed on day 4 when the outdoor temperature readings were highest (Figure 13).

Passive setup in the cooling season: week 3

During week 3, 8–14 July, the environmental control facility was disconnected to assess TTW passive behaviour in the summer.

Surface temperature

In this case also (Figure 14), TTW surface temperature and the other monitoring data followed very similar patterns. The outdoor temperature in week 3 ranged from

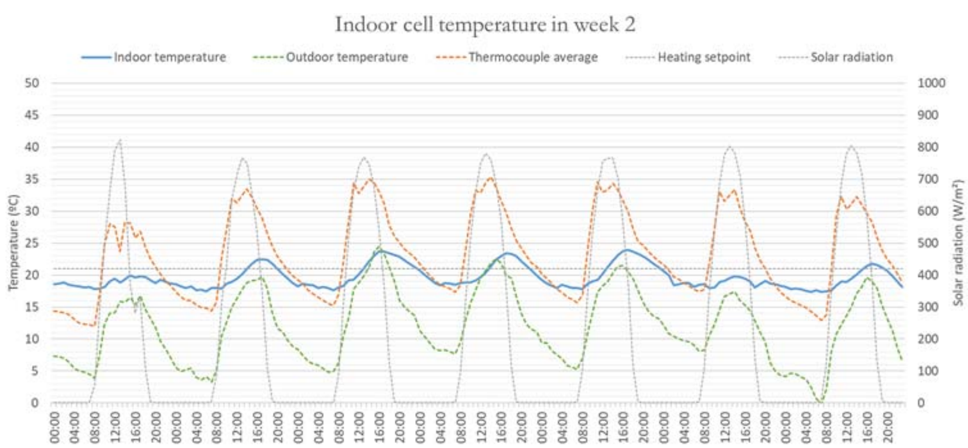

Figure 12. Indoor cell temperature in week 2.

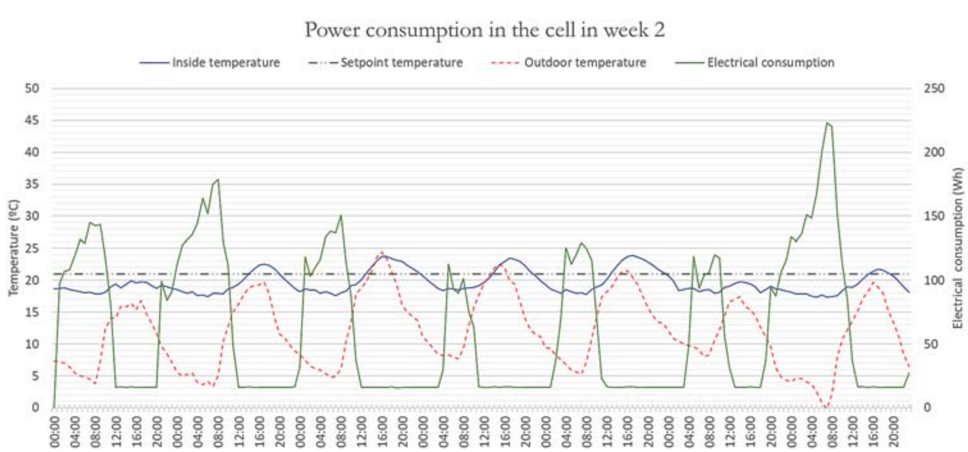

Figure 13. Power consumption in the cell in week 2.

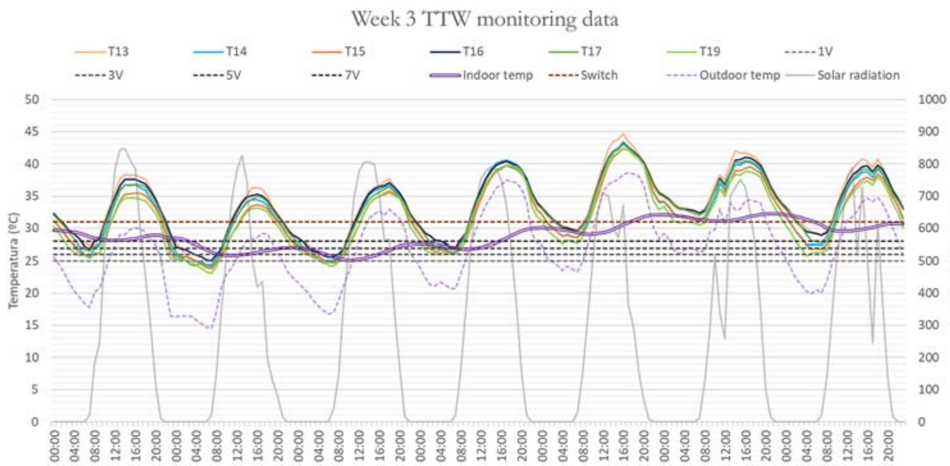

Figure 14. Week 3 TTW monitoring data.

14.6°C to 38.6°C, for a mean of 27°C. Mean maximum daily solar radiation was 788.8 W/m^2, similar to the week 2 value. The mean temperature recorded by the thermocouples was 32.7°C. The highest means were found for mid-height T13 at 33.7°C and upper wall T16 at 33.4°C. The highest surface readings were recorded by thermocouples T13 (44.7°C) and T14 (43.4°C), although the difference to the overall maximum mean, 43.2°C, was less pronounced than in week 2. Peak temperature was reached in all the thermocouples at 16:00 on day 5, when radiation was lowest but the outdoor temperature highest (Figure 14).

The mortar surface exceeded the Tc after 9:00, 10:00, 11:00 or 12:00, depending on the day and area of the wall. Since on day 6 the surface temperature was no lower than 31°C, the failure of TCC to change colour at under the Tc during that week was deemed scantly significant. Mortar behaviour was very similar to that of a colourless wall with a constant, uniform optical response and high reflectance. More specifically, the visible absorptance was 0.47 and the solar value 0.36. Here also, the outdoor temperature was observed to have a greater impact than solar radiation on TCC surface temperature. Even though peaks were recorded, the mean daily difference between the surface and outdoor temperatures was just 5.7°C, compared to 7.4°C in week 1 and 11.2°C in week 2.

Air velocity in the air gap

In week 3, the mean air velocity reading at A2 was 0.8 m/s and at A3 0.9 m/s, much higher than in the two other weeks studied. The maxima were 0.15 m/s (A2) and 0.12 m/s (A3), although they were barely perceptible given the constant fluctuations recorded. Solar radiation was not visibly related to the increase in air velocity in the air space, given the 'summer' setting in the vents. The anemometers values were affected less by circulation inside the space than by the outdoor air flowing into it across the window vents to expel the warm air accumulating there. That, together with fan operation (95% of the time), would explain the high air velocity in the air space (Figure 15).

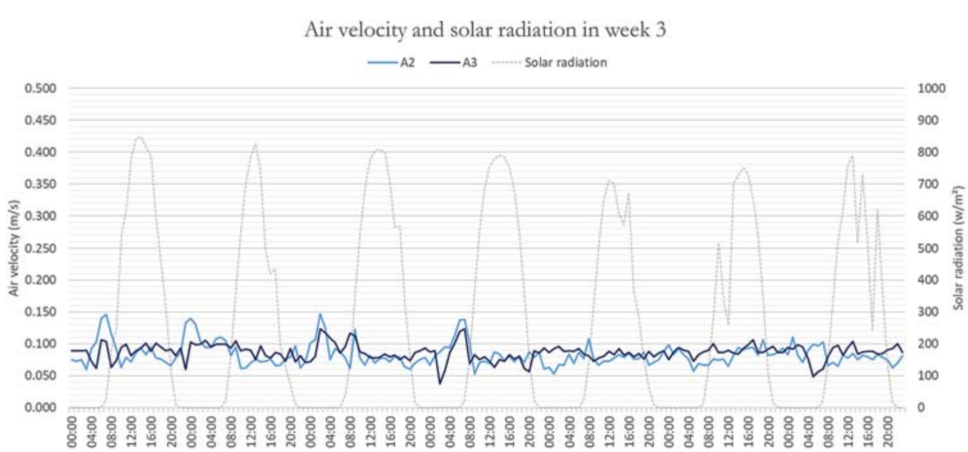

Figure 15. Air velocity and solar radiation in week 3.

Indoor vs outdoor temperatures

Temperatures were considerably warmer in week 3 than in weeks 1 and 2, with an outdoor mean of 28.9°C and an indoor value of 27°C. As in the other two weeks, the TTW mitigated indoor fluctuations, with significantly less steep peaks and valleys than in the outdoor and wall temperatures. Outdoor values ranged from 14.6°C to 38.6°C, whereas indoors the interval fluctuated from a minimum of 25.1°C to a maximum of 32.2°C (Figure 16).

Slight overheating was observed inside the module to the detriment of prototype summertime performance. Due to the airtightness of the indoor area, indoor temperature fluctuation was much less accentuated and substantially delayed relative to outdoor conditions. Overheating could be remedied with natural night time ventilation to reduce the higher indoor temperatures in the cell attributable in part to the thermal mass of the construction elements. Whilst the TTW reduced overheating, it afforded only 2 extra hours of comfortable temperatures. Nonetheless, DDH was brought down by 39.5%, denoting substantially better performance than observed in wintertime week 1 (15%). If the system's indoor and outdoor vents had been opened during the night to release the warm air accumulating inside the cell, the DDH value could have been lowered even further.

By way of a general observation applicable to three weeks analysed, the presence of occupants and the use of lighting or other appliances, not taken into consideration in this experiment, would raise the indoor temperature, to the benefit of winter time and detriment of summer time comfort levels.

Simulation model validation with experimental data

Model validation with the data gathered here will be the object of a future study. That will entail processing larger volumes of data and addressing the complexity involved in simulating the dynamic behaviour of chromogenic materials, studied earlier by both Favoino (Favoino et al., 2017) and Loonen (Loonen et al., 2017). For the present intents and purposes, however, the stable conditions observed in weeks 1 and 3 are analysed in the following discussion on the grounds of seasonal rather than daily thermal-optical changes with a simulation model developed earlier.

As the thermocouples did not exceed the activation temperature in week 1, the thermochromic mortar remained coloured throughout. Conversely, in week 3 the mortar remained colourless. Those two findings were used to conduct a 'non-dynamic' analysis with Energy Plus open code software that simulates building energy consumption and thermal loads. *Design builder* software was the user interface applied for data entry and output data.

The data were analysed at 1 h intervals. The weather data recorded at the in situ meteo station in the periods studied were compiled in '.epw' (Energy Plus Weather) format to define the outdoor conditions for the simulation. The module's geometric and thermal optical properties were defined using *Design builder*. The only output analysed, indoor temperature, was compared to the interior temperature recorded by the in-cell sensor in the two weeks analysed.

Borrowing on methodology published in a recent study (Camacho-Montano et al., 2020), the observed and predicted values were compared based on the coefficient of variation of the root mean square error (CVRMSE). ASHRAE deems a difference of up to ±30% for a hourly calibration data to be acceptable (ASHRAE, 2002). In the winter week the mean CVRMSE was 18%, however, and the difference on days 3 (32%) and 4 (29%) (Figure 17) indicated considerable discrepancy between the results. Disregarding

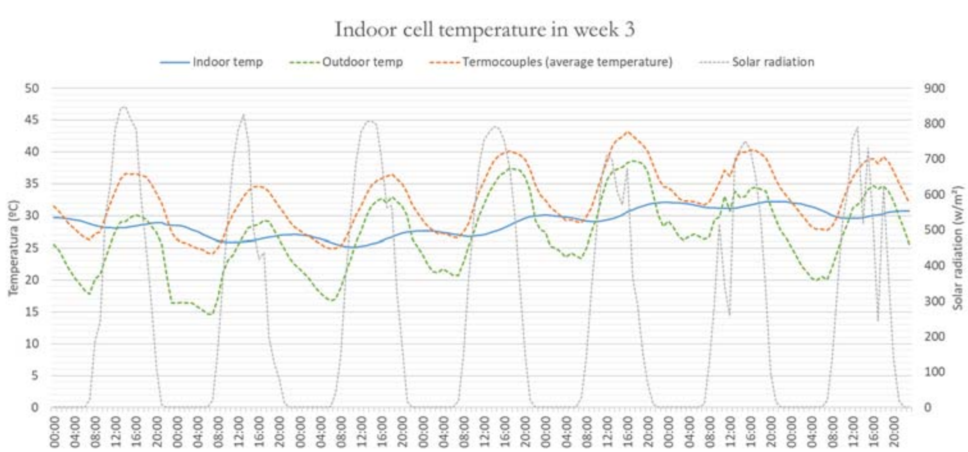

Figure 16. Indoor cell temperature in week 3.

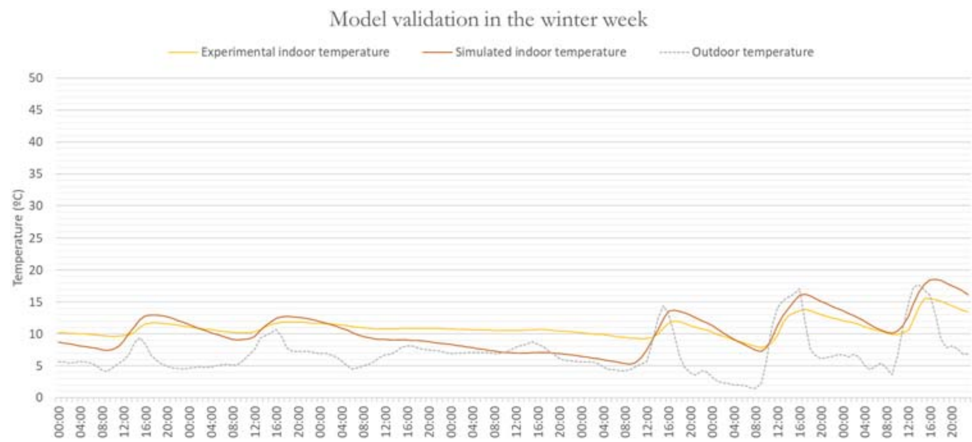

Figure 17. Model validation in the winter week.

those two outliers, however, yielded a mean CVRMSE of ≤13%. The summertime mean CVRMSE was only 3% (Figure 18), denoting very close agreement between the measured and simulated values.

In light of the validation findings, the model was deemed appropriate to compare TCC performance to three types of conventional cladding: the usual black paint and, to simulate the TCC cladding when colourless and coloured, grey and colourless cladding. In other words, the latter two did not change tone with temperature; the colourless panels remained colourless at low temperatures and the grey panel grey at high temperature (Table 5). The comparison aimed to verify the advantages of TCC thermochromism.

Only a narrow difference was observed in the summertime surface temperature between the TCC and the permanently coloured cladding. The values for the former were 0.2°C lower on average, hour by hour, with a maximum difference of 0.5°C. The temperature in the TCC was a full 1°C lower hourly and a maximum 2.4°C lower than in the conventional black cladding. In winter the TCC exhibited a mean 0.4°C higher temperature, hour by hour, and a maximum 1.5°C higher than the permanently colourless material. The TCC obviously did not heat to the temperatures recorded for the black cladding, which was a mean hourly 1.8°C warmer with the difference peaking at 7.2°C (Figure 19).

The indoor temperatures recorded for the two simulated claddings exhibited narrower differences (Figure 20). TCC performance was similar to that recorded for both, at a mean hourly difference of 0.1°C. The difference between TCC and the conventional black cladding was considerably wider, however, in both winter and summer, with the latter exhibiting 0.7°C higher mean hourly temperatures. As Figure 20 shows, however, the maximum difference was greater in the winter, at 2°C, than in the summer, when it was 1.3°C. In terms of the comfort ranges defined in the methodology, 2% more DDH was observed in winter for the non-thermochromic cladding than for the TCC. The conventional cladding delivered the greatest wintertime comfort, with 7% fewer DDH than the

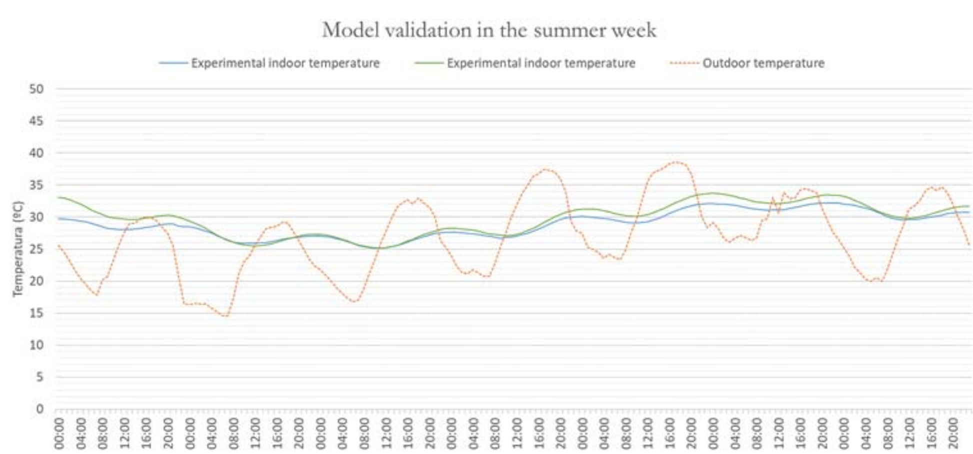

Figure 18. Model validation in the summer week.

Table 5. Optical properties of simulated mortars.

	Colourless		Coloured	
	Solar	Visible	Solar	Visible
TCC	0.36	0.47	0.43	0.58
Dark grey	0.43	0.58	0.43	0.58
Light beige	0.36	0.47	0.36	0.47
Black	0.90	0.90	0.90	0.90

TCC. In the summertime, however, it exhibited 16% more DDH than the permanently grey and colourless cladding and 19% more than the TCC.

Through the simulation carried out, the need to widen the difference in the absorptance / reflectance coefficients between both states of the TCC (coloured and colourless) can be prioritized to improve the thermal performance of the TTW. A TCC whose colour state is closer to black and its colourless state is closer to white, will be able to obtain the thermal benefits of a black cladding, although avoiding the penalties generated in the cooling season. Through the DDH obtained, it is shown that, in an annual overview, the conventionally used black paint entails greater harm than good for the comfort of the inhabitant.

Conclusions

This article describes a full-scale experiment conducted to determine the thermal performance of a prototype Trombe wall designed to vary its optical properties with temperature. The reversible rise in the reflectance of thermochromic cladding (TCC), here at an activation temperature (Tc) of 31°C, lowers the heat accumulating in such walls to improve performance in regions with warm summers. Since the activation temperature may also be reached on sunny winter days, however, an experimental system to cool the TCC under controlled conditions was also tested.

The data to characterize TTW behaviour were collected with temperature sensors on the TCC surface and inside the experimental cell, as well as anemometers to measure air flow velocity in the Trombe wall air space.

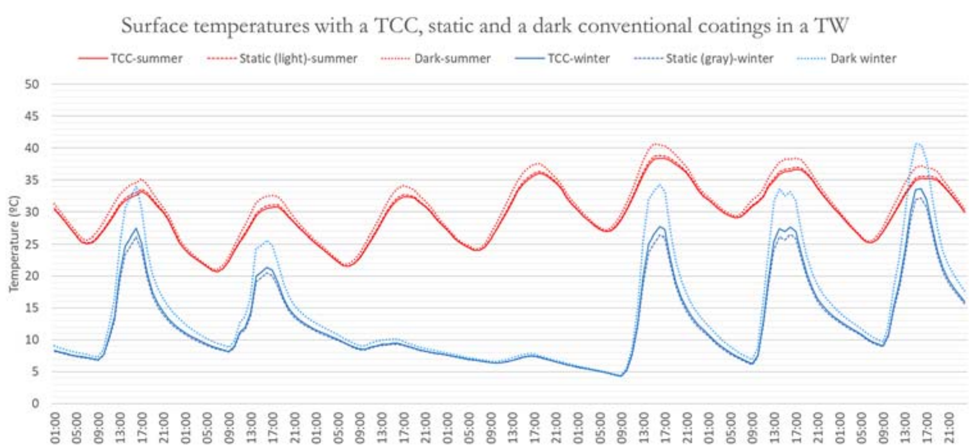

Figure 19. Comparison of surface temperatures in a thermochromic and a conventional mortar in a TW.

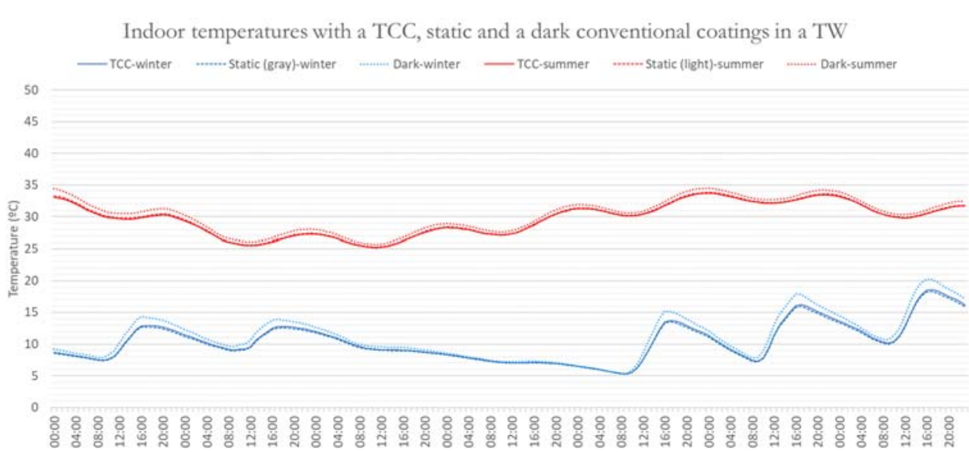

Figure 20. Comparison of indoor temperatures in a thermochromic and a conventional mortar in a TW.

The differences observed in the temperatures recorded by the surface thermocouples in the winter, with indoor-indoor air flow, were attributable to air temperature inside the space, which increased as the air rose from bottom up. In the late winter and summer weeks analysed, those differences were also due to the shade projected over part of the wall by the eaves on the cell, which determined variations in thermocouple exposure to solar rays or, in late winter, to their proximity to or distance from the vents through which the air entered the pocket.

The 200 ach ventilation provided by seven fans installed near the bottom of the air space prevented the TCC from fading when the Tc was exceeded in winter.

A comparison of the outside air to the TCC surface temperature afforded a measure of the capacity of the cladding to radiate and absorb heat. Its thermal inertia mitigated the abrupt declines in outdoor wintertime temperatures. In the summer, outdoor-outdoor air circulation was enhanced by opening the vents, which raised the ventilation rate by 67%, for faster release of the heat accumulated in the TCC.

Gauged against pre-defined thermal comfort ranges, the TCC system reduced summertime DDH by 39.5% relative to the conventional TW and wintertime DDH by 15%.

Active heating was deployed to maintain comfortable indoor temperatures in the spring. Energy consumption was indirectly proportional to the outdoor temperature, rising as the weather cooled, for a mean of 64.44 kWh.

Dynamic material simulation will be addressed in future research. Nonetheless, as this experiment showed that in summer and winter the TCC remained essentially colourless or coloured, respectively, the simulated data could be acceptably validated against the observed findings using CVMRSE techniques. The model was used to compare the TCC with black, grey and colourless conventional cladding. TCC delivered slightly cooler summertime and warmer wintertime temperatures than the conventional grey and colourless material sand performed even better compared to the black conventional cladding. Although the latter obviously absorbed more heat, providing for 7% more hours of wintertime comfort, that was greatly offset by the 19% improvement in summertime indoor temperatures afforded by the TCC system.

By way of summary, further to the present findings thermochromic materials such as the TCC studied here can feasibly be used in Trombe wall systems to improve year-round performance in climates with warm summers. For greater efficacy, however, the difference between the coloured and colourless optical ranges must be widened, seeking conditions comparable to the white (all wavelengths of visible light)-black (absence of visible light) extremes.

Possible improvements to be addressed in future include greater differences between coloured and colourless TCC absorptance, higher insulating power of the outer glass to reduce wintertime loss and summertime gain, night time cell ventilation to enhance warm season cooling and automatic vent operation based on weather conditions and the sun's path.

In addition to those improvements, research could address the most suitable ventilation for the TTW. This study explored the vent setup that would deliver indoor-indoor air flow in winter (TW) or outdoor-outdoor flow in summer (ventilated façade). Indoor-outdoor strategies may also be researched, however. A winter time study of a thermally massive wall is proposed to estimate the capacity of the TTW to pre-heat the outdoor air before it flows indoors or to dispense with mechanical ventilation to prevent the TCC change from coloured to colourless. The use of a solar chimney in summer might be analysed, drawing warm indoor air from the wall by opening the vents at the bottom of the wall and the top of the window.

The present promising findings contribute to furthering the application of and research on chromogenic materials in building energy refurbishment.

Acknowledgements

This research was supported by the grants from Ministry of Economy and Competitiveness of Spain, under the Project BIA2014-56827R, and from the CSIC in the i-Link + 2019 call under the project LINKA20220 Project 'Nanotechnology - based thermochromic materials for adaptive building envelopes' (2020-2021). Funding was also received from Mexico's National Council of Science and Technology (CONACYT) and the foundation of the National Institute of Fine Arts (FINBA). The support provided by the Spanish Meteorological State Agency (AEMET) in the form of data is gratefully acknowledged.

Disclosure statement

No potential conflict of interest was reported by the author(s).

Funding

This research was supported by the grants from Ministry of Economy and Competitiveness of Spain [Project BIA2014-56827R], and from the CSIC in the i-Link + 2019 call under the project LINKA20220 Project 'Nanotechnology-based thermochromic materials for adaptive building envelopes' (2020–2021). Funding was also received from Mexico's National Council of Science and Technology (CONACYT) and the Foundation of the National Institute of Fine Arts (FINBA).

ORCID

Arturo Martínez http://orcid.org/0000-0002-3384-4061
Carmen Alonso http://orcid.org/0000-0002-5606-9950
Fernando Martín-Consuegra http://orcid.org/0000-0002-2714-6910
Gloria Pérez http://orcid.org/0000-0001-9268-5964
Borja Frutos http://orcid.org/0000-0002-6969-1722
Álvaro Gutiérrez http://orcid.org/0000-0001-8926-5328

References

ASHRAE Guideline 14. (2002). *Measurement of energy and demand savings*. American Society of Heating, Refrigerating and Air-Conditioning Engineers.

Baetens, R., Jelle, B. P., & Gustavsen, A. (2010). Properties, requirements and possibilities of smart windows for dynamic daylight and solar energy control in buildings: A state-of-the-art review. *Solar Energy Materials and Solar Cells*, *94*(2), 87–105. https://doi.org/10.1016/j.solmat.2009.08.021

Bajc, T., Todorović, M. N., & Svorcan, J. (2015). CFD analyses for passive house with Trombe wall and impact to energy demand. *Energy and Buildings*, *98*, 39–44. https://doi.org/10.1016/j.enbuild.2014.11.018

Beck, A., Hoffmann, T., Körner, W., & Fricke, J. (1993). Thermochromic gels for control of insolation. *Solar Energy*, *50*(5), 407–414. https://doi.org/10.1016/0038-092X(93)90061-R

Bellos, E., Tzivanidis, C., Zisopoulou, E., Mitsopoulos, G., & Antonopoulos, K. A. (2016). An innovative Trombe wall as a passive heating system for a building in Athens – a comparison with the conventional Trombe wall and the insulated wall. *Energy and Buildings*, *133*, 754–769. https://doi.org/10.1016/j.enbuild.2016.10.035

Bevilacqua, P., Benevento, F., Bruno, R., & Arcuri, N. (2019). Are Trombe walls suitable passive systems for the reduction of the yearly building energy requirements? *Energy*, *185*, 554–566. https://doi.org/10.1016/j.energy.2019.07.003

Camacho-Montano, S. C., Cook, M., & Wagner, A. (2020). Avoiding overheating in existing school buildings through optimized passive measures. *Building Research and Information*, *48*(4), 349–363. https://doi.org/10.1080/09613218.2019.1663137

Dabaieh, M., & Elbably, A. (2015). Ventilated Trombe wall as a passive solar heating and cooling retrofitting approach; a low-tech design for off-grid settlements in semi-arid climates. *Solar Energy*, *122*, 820–833. https://doi.org/10.1016/j.solener.2015.10.005

Directive 2012/27/EU on energy efficiency. *Official Journal of the European Union*. https://eur-lex.europa.eu/legal-content/EN/TXT/PDF/?uri=CELEX:32018L0844&from=EN

European Parliament and of the Council. (2014, June 30). Directive (EU) 2018/844 of the European Parliament and of the Council of 30 May 2018 amending directive 2010/31/EU on the energy performance of buildings and European Commission. (2019). Recomendación de la comisión de 7.6.2019 relativa a la modernización de edificios. *Official Journal of the European Union*. https://www.boe.es/doue/2019/165/L00070-00128.pdf

Fabiani, C., Castaldo, V. L., & Pisello, A. L. (2020). Thermochromic materials for indoor thermal comfort improvement: Finite difference modeling and validation in a real case-study building. *Applied Energy*, *262*, 1–17. https://doi.org/10.1016/j.apenergy.2019.114147

Favoino, F., Giovannini, L., & Loonen, R. (2017, November). Smart glazing in intelligent buildings: what can we simulate? *GPD 2017 – Glass Performance Days* 2017, 8–15. https://www.researchgate.net/publication/321019036

Garshasbi, S., & Santamouris, M. (2019). Using advanced thermochromic technologies in the built environment: Recent development and potential to decrease the energy consumption and fight urban overheating. *Solar Energy Materials and Solar Cells*, *191*, 21–32. https://doi.org/10.1016/j.solmat.2018.10.023

Gavira, M., Perez, G., & Acha, C. (2018). Estudio comparativo del efecto de las propiedades ópticas del revestimiento exterior de fachada sobre la demanda energética de un edificio. *Dyna*, *93*(1), 216–220. https://doi.org/10.6036/8487

Hernández-López, I., Xamán, J., Chávez, Y., Hernández-Pérez, I., & Alvarado-Juárez, R. (2016). Thermal energy storage and losses in a room-Trombe wall system located in Mexico. *Energy*, *109*, 512–524. https://doi.org/10.1016/j.energy.2016.04.122

Liu, Y., Wang, D., Ma, C., & Liu, J. (2013). A numerical and experimental analysis of the air vent management and heat storage characteristics of a Trombe wall. *Solar Energy*, *91*, 1–10. https://doi.org/10.1016/j.solener.2013.01.016

Loonen, R. C. G. M., Favoino, F., Hensen, J. L. M., & Overend, M. (2017). Review of current status, requirements and opportunities for building performance simulation of adaptive facades. *Journal of Building Performance Simulation*, *10*(2), 205–223. https://doi.org/10.1080/19401493.2016.1152303

Martín-Consuegra, F., Alonso, C., Perez, G., Guerrero, A., Gavira, M. J., Frutos, B., & Oteiza, I. (2019). Design and optimisation of a thermochromic Trombe wall. In *International Conference on Sustainable Materials, Systems and Structures (SMSS 2019) Energy Efficient Building Design and Legislation* (pp. 42–50). RILEM Publications SARL.

Nayak, J. K. (1987). Transwall versus Trombe wall: Relative performance studies. *Energy Conversion and Management*, *27*(4), 389–393. https://doi.org/10.1016/0196-8904(87)90117-8

Perez, G., Allegro, V. R., Alonso, C., Martín-Consuegra, F., Oteiza, I., Frutos, B., & Guerrero, A. (2019). Selection of suitable materials for the development of an innovative thermochromic Trombe wall. *Advances in Building Energy Research*, 1–15. https://doi.org/10.1080/17512549.2019.1684364

Perez, G., Allegro, V. R., Corroto, M., Pons, A., & Guerrero, A. (2018). Smart reversible thermochromic mortar for improvement of energy efficiency in buildings. *Construction and Building Materials*, *186*, 884–891. https://doi.org/10.1016/j.conbuildmat.2018.07.246

Pittaluga, M. (2013). The electrochromic wall. *Energy & Buildings*, *66*, 49–56. https://doi.org/10.1016/j.enbuild.2013.07.028

Reynisson, H. E., & Guðmundsson, K. (2015). *Energy performance of dynamic windows in different climates* [Master's Thesis, Sweden School of Architecture and the Built Environment Division of Building Technology]. Available at: KTH´s Publication data base DiVA, retrieved from http://kth.diva-portal.org/smash/record.jsf?pid=diva2%3A825465&dswid=28

Stazi, F., Mastrucci, A., & Di Perna, C. (2012). The behaviour of solar walls in residential buildings with different insulation levels: An experimental and numerical study. *Energy and Buildings*, *47*, 217–229. https://doi.org/10.1016/j.enbuild.2011.11.039

Zalewski, L., Joulin, A., Lassue, S., Dutil, Y., & Rousse, D. (2012). Experimental study of small-scale solar wall integrating phase change material. *Solar Energy*, *86*(1), 208–219. https://doi.org/10.1016/j.solener.2011.09.026

Zinzi, M. (2016). Characterisation and assessment of near infrared reflective paintings for building facade applications. *Energy & Buildings*, *114*, 206–213. https://doi.org/10.1016/j.enbuild.2015.05.048